

## Backward Scattering in the Reaction $\pi^- p \rightarrow \rho^0 \pi^- p$ at 5 GeV/c\*

B. C. Harms and S. T. Jones

University of Alabama, University, Alabama 35486

(Received 10 April 1972)

Two models for backward pion-proton scattering are used in an investigation of nonperipheral events in the process  $\pi^- p \rightarrow \rho^0 \pi^- p$ . A multi-Regge model, incorporating baryon and pion exchange, is found to reproduce angular distributions well, but does a poor job describing invariant masses. A second model, incorporating on-shell pion-nucleon phase shifts, fits all aspects of the data. Pion exchange in both models is well supported. Speculations regarding inclusive reactions stress the inadequacy of single-particle spectra in distinguishing between different models.

### I. INTRODUCTION

We have undertaken a study of nonperipheral events in the reaction  $\pi^- p \rightarrow \rho^0 \pi^- p$  at 5 GeV/c, with the purpose of analyzing the predictions of two contrasting models. We have chosen this reaction because of the availability of a relatively large amount of data, and have focused our attention on those events in which the proton is not highly peripheral. We have compared these events to a model involving baryon exchange and a model involving off-shell  $\pi^- p$  scattering. These two models are fundamentally different in their composition and predictions, and we expect *a priori* that the second is the one likely to best reproduce the over-all behavior of the data. Nevertheless, there has been increased use of baryon exchange in recent phenomenological and theoretical models, with some success, and we have attempted to determine the extent to which we could rely on this mechanism.

Recent inclusive experimental data<sup>1</sup> has shown rather surprising persistence of nonperipheral protons. For example, the distribution in  $p_L$  for secondary protons in  $pp \rightarrow p + X$  (unobserved) is quite flat in the center of mass. Fits to this inclusive data have used significant contributions from Reggeized baryon exchange, though in a many-parameter model.<sup>2</sup> Also in the inclusive regime, models for deep-inelastic electron-proton scattering have been proposed which are based on multiple baryon exchange.<sup>3</sup> Finally, in a study of an inclusive reaction, Ajduk *et al.*<sup>4</sup> found that baryon exchange, in the context of the C $\bar{L}$ A (Chan-Loskiewicz-Allison) model,<sup>5</sup> accounted for close to half of the observed cross section, and that the region covered by single baryon exchange overlaps significantly the region in which multiperipheral models (*no* baryon exchange) were thought to predominate.

In the analysis of Risk and Friedman,<sup>2</sup> it was found that a single baryon exchange was sufficient

to describe the existing data. Coupled with the assumption of pion exchange and pion production, this portion of their model takes on the appearance of off-shell pion-proton scattering, as indicated in Fig. 1. An improved description of this graph is obtained if we replace the baryon exchange  $\pi^- p$  amplitude by the on-shell  $\pi^- p$  amplitude. In this paper we wish to make a comparison of these two alternative descriptions, by applying them to an *exclusive* process. This exclusive process corresponds to the case where the unobserved  $X$  in Fig. 1 is just a  $\rho$  meson. Extrapolation from our analysis to the inclusive process is unreliable, and we consider the important results of our work to be primarily the demonstration of the relative abilities of the two models to describe the nonperipheral exclusive data at hand. However, we do speculate that our conclusions are meaningful in a limited way in the inclusive regime.

The data which we have analyzed were obtained from the University of Illinois high-energy group.<sup>6</sup> Additional data of theirs at 7 GeV/c were used in one part of the analysis.

We describe the fits of the models to the data in Secs. II-IV, and we compare the results of the fits in Sec. V.

### II. BARYON EXCHANGE MODEL

Our double-Regge model and the pertinent variables are described graphically in Fig. 2. We have pion and  $\Delta_\delta$  Regge exchanges, and our amplitude is written

$$M = f_{\text{BW}}(m_{\pi^+ \pi^-}, \theta_1) P_1(t, S_{\rho\rho}) P_2(u, S_{\pi^- p}), \quad (1)$$

where  $f_{\text{BW}}$  is a relativistic Breit-Wigner form of the Jackson type,<sup>7</sup> and  $P_1$  and  $P_2$  are Regge propagators;

$$S_{ab} = (p_a + p_b)^2,$$

$$t = (p_1 - q_1 - q_2)^2,$$

$$u = (p_2 - q_4)^2.$$

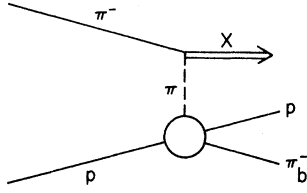


FIG. 1. Diagram used to account for nonperipheral protons. In the inclusive process,  $X$  is anything, and its mass varies over the allowed phase space. In this study,  $X$  is a  $\pi^+\pi^-$  system with mass in the  $\rho$  region. The process studied in Ref. 2 was  $p\bar{p} \rightarrow pX$ , and the model used was described in part by a diagram analogous to this.

Specifically,

$$P_1 = \frac{1}{4}\pi(\alpha_\pi + 2) \left( \frac{1 + e^{-i\pi\alpha_\pi}}{\sin\pi\alpha_\pi} \right) \left( \frac{S_{\rho p}}{S_1} \right)^{\alpha_\pi}, \quad (2)$$

with  $\alpha_\pi = t - m_\pi^2$ . We have included the factor  $(\alpha_\pi + 2)$  to eliminate the ghost at  $t \approx -2$ , which is otherwise noticeable even at  $t \approx -1.0$ , for the particular values of the scale parameter  $S_1$  which we found appropriate. The propagator  $P_2$  is actually represented in our model by virtual  $\pi^-p$  scattering, so that full account of proton spin is taken. The specific form for the usual  $A$  and  $B$  amplitudes, taken from Berger and Fox,<sup>8</sup> is

$$A = -\frac{1}{2}\pi \frac{(1 + \tau e^{-i\pi\bar{\alpha}})}{\Gamma(1 + \bar{\alpha}) \sin\pi\bar{\alpha}} \gamma_A(u) \left( \frac{S_{\pi p}}{S_2} \right)^{\bar{\alpha}}, \quad (3)$$

$$B = -\frac{1}{2}\pi \frac{(1 + \tau e^{-i\pi\bar{\alpha}})}{\Gamma(1 + \bar{\alpha}) \sin\pi\bar{\alpha}} \gamma_B(u) \left( \frac{S_{\pi p}}{S_2} \right)^{\bar{\alpha}}.$$

The residues  $\gamma_A$  and  $\gamma_B$  are parametrized linearly as in Ref. 8;  $\bar{\alpha} = \alpha_\Delta - \frac{1}{2} = 0.9u - 0.5$ ; and  $\tau = -1$ . We have kept the same parameters found by Berger and Fox, except that the scale parameter  $S_2$  was varied in order to fit the observed distribution in the proton scattering angle  $\theta_{pp}$ . Variation in  $S_2$  without compensating changes in the normalization ( $\gamma$ ) means that we no longer satisfy constraints at the  $\Delta$  pole ( $\alpha_\Delta = \frac{3}{2}$ ). For example, the width of the  $\Delta(1236)$  is given by<sup>8</sup>

$$\Gamma_\Delta = \frac{(E_\Delta + m_N) q_\Delta^3}{12\pi b S_2 m_\Delta^2} \gamma_\Delta(m_\Delta), \quad (4)$$

with

$$\gamma_\Delta = \gamma_A(u) - (\sqrt{u} - m_N) \gamma_B(u). \quad (5)$$

$b$  is the slope of the  $\Delta_\delta$  trajectory;  $b = 0.9 \text{ GeV}^{-2}$ . We cannot simultaneously satisfy this constraint and fit the shape of the present data. We have *not* attempted to adjust  $\gamma_\Delta$  concurrently with  $S_2$  in accordance with Eq. (4) but have allowed this constraint to slide. Deviation of  $\gamma$  from linearity beyond the physical region can restore this constraint.

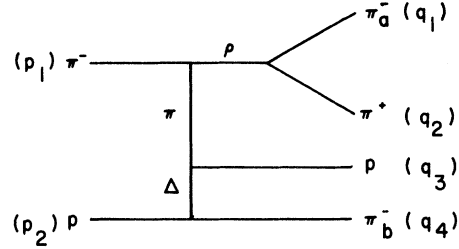


FIG. 2. Baryon-exchange diagram. The variables assigned to the 4-momenta for each particle are in parentheses.

The parameters  $S_1$  and  $S_2$  were set at  $10.0 \text{ GeV}^2$  and  $4.0 \text{ GeV}^2$ , respectively. Both these values are quite high, as Regge parameters go.  $S_1$  was adjusted to approximately fit the experimental distribution in  $t$ , and had to be set large because the  $t$  slope is so flat in the region of interest. Berger and Fox<sup>8</sup> found  $S_2 = 1.1 \text{ GeV}^2$  for elastic scattering, but again we are forced to higher values because the backward peak in the proton-scattering angle  $\theta_{pp}$  (in the  $\pi^-p$  center-of-mass system) is quite small experimentally. Our value of  $S_2$  also improves the  $\pi^-p$  mass spectrum considerably.

It should be noted that the Regge model does not fit backward *elastic* scattering at the low subenergies important here. Use of Regge exchange in this instance relies, then, on the validity of duality in the multiparticle regime. Nevertheless, we might expect some success in our application of the multi-Regge model, judging from the success of (1) previous applications involving meson exchanges,<sup>9</sup> and (2) fits to proton distributions in inclusive reactions using Reggeized baryon exchange.<sup>2</sup>

The  $\rho^0$ -decay distribution was given the form  $a + b \cos^2\theta$ , to take into account nonresonant ( $s$ -wave) events. The observed distribution was then fitted with  $a = 0.25$ ,  $b = 0.75$ . Our primary concern here was to fit as well as possible the  $\rho$  region, which is much better understood than other regions of the  $\pi^+\pi^-$  spectrum. Our theoretical interest is focused on the details of the  $\pi^-p$  vertex, and it is therefore desirable that we not have to worry excessively about details of the other ( $\rho$ ) vertex.

No provision was made for off-shell effects of the two-body scattering (form factors). These effects are simulated by the residue function in the Regge propagator, and variation of the scale parameter  $S_1$  gives adequate representation of the data.

The normalization of our model raises a difficult problem. As mentioned above, variation of the parameter  $S_2$  without compensating changes in  $\gamma_\Delta$  destroys our normalization at the  $\Delta(1236)$  pole,

but is necessary in order to fit the data. With the current parameters, we find a total cross section for the reaction  $\pi^- p \rightarrow \rho^0 p \pi^-$ , with only the restriction  $|t| < 1.0$ , of  $\sigma = 0.75$  mb, which is well above the experimental value. Adjustment of  $\gamma_\Delta$  to compensate for the change in  $S_2$  would increase this by a factor of about 13, and is clearly unacceptable. The dependence of  $\sigma$  on the parameters  $S_1$  and  $S_2$  is not insignificant, particularly in the latter case, but is not sufficient to decrease  $\sigma$  by the factor of 4 or 5 necessary to provide agreement with the data in the backward region. Problems of normalization are unfortunately quite common to multi-peripheral models, and we consider the most important test of our present model to be its comparison to the *shape* of the data.

### III. COMPARISON OF BARYON-EXCHANGE MODEL WITH THE DATA

The data we have used consist of 13 858 events of the type  $\pi^- p \rightarrow \pi^+ \pi^- \pi^- p$  at 5 GeV/c. As will be seen in the figures, only a small percentage of these events can be readily associated with our model. In fact, only 3660 events survive the three cuts made to isolate events of the type  $\pi^- p \rightarrow \rho^0 \pi^- p$  with pion exchange (see Fig. 3). When an additional four cuts are made to isolate the baryon-exchange region, only 314 events remain in the data. We have taken the total cross section for  $\pi^- p \rightarrow \pi^+ \pi^- \pi^- p$  to be 1.8 mb at 5 GeV/c; thus these two subsamples (discussed below) have cross sections of 0.48 mb and 0.041 mb, respectively.

Calculations for the theoretical distributions were done by Monte Carlo generation, and our

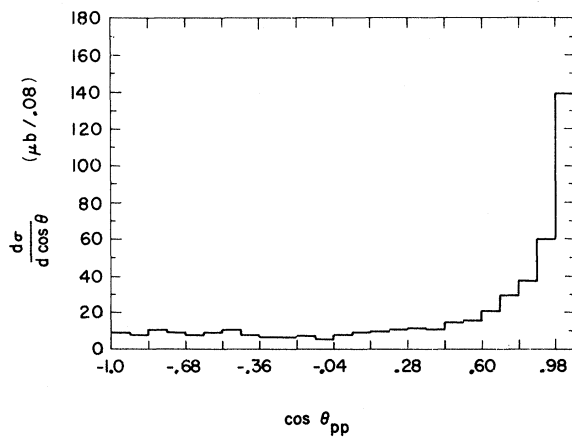


FIG. 3. Distribution in  $\cos \theta_{pp}$ , where  $\theta_{pp}$  is the angle between initial and final protons in the  $(\pi^-_i p)$  rest frame. Only three cuts have been applied, as explained in the text.

curves have been smoothed slightly by hand.

In order to isolate the events of the type shown in Fig. 2, several cuts were made on the data. Figure 3 is a plot of the cosine of the angle ( $\theta_{pp}$ ) between the initial (target) proton and the final proton as measured in the  $(\text{proton}, \pi^-_b)$  system with the following cuts:

$$(1) 0.65 \text{ GeV}/c^2 \leq m_{\pi^+ \pi^-} \leq 0.85 \text{ GeV}/c^2.$$

Here  $a$  ( $b$ ) signifies the  $\pi^-$  in (not in) the  $\rho$ , respectively. If both  $\pi^+ \pi^-$  effective-mass combinations were in the  $\rho$  region, the event was entered twice into each plot with a weight of  $\frac{1}{2}$  for each entry. In addition, we require

$$(2) |t| < 1 \text{ (GeV}/c)^2$$

and

$$(3) \text{ no } \Delta^{++}(1236).$$

A backward peak in  $\cos \theta_{pp}$  is not clearly present at this point, indicating the dominance of peripheral mechanisms in this sample of events.

The sample of events was further restricted to those events with  $u \geq 0.0$   $(\text{GeV}/c)^2$  and  $\cos \theta_{pp} \leq 0.0$ , and the  $\Delta^0(1236)$  was removed by making a window cut on the  $p\pi^-$  system. This cut was made to remove a cluster of resonant events in the region

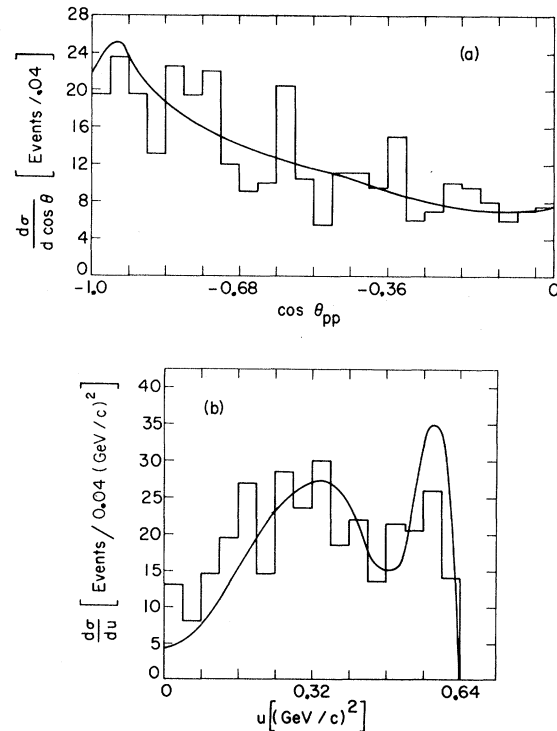


FIG. 4. Comparison of baryon-exchange model and data, with seven cuts applied (see text): Distribution as a function of (a)  $\cos \theta_{pp}$ , and (b)  $u$ .

$$1.15 \text{ GeV}/c^2 \leq m(p\pi_b^-) \leq 1.35 \text{ GeV}/c^2$$

and

$$0.04 (\text{GeV}/c)^2 \leq |t| \leq 0.3 (\text{GeV}/c)^2.$$

Finally, events with

$$1.62 \text{ GeV}/c^2 \leq m(p\pi_b^-) \leq 1.76 \text{ GeV}/c^2$$

were removed to eliminate the  $N^*(1690)$ . These cuts were made with the intention of eliminating effects we knew the model could not reproduce, at a cost of removing most of the data. We believe this approach gives the most leeway to the model, which we know can give only a limited description of the physical situation.

The baryon-exchange model can be adjusted to give adequate representation of the data in most respects, the important exception being the  $(\pi^-p)$  mass distribution. Representative fits to variables of interest here are given in Figs. 4–6. In these figures, the predictions of the model have been normalized to the data. It is significant to us that the angular distributions,  $\cos\theta_{pp}$  and  $u$ , are well described by the model, and that the longitudinal momenta (Fig. 5) are adequately described. The large dips in the distributions in all these figures (both in experimental and theoretical curves) are due to the removal of the  $\Delta^0(1236)$  events. The ap-

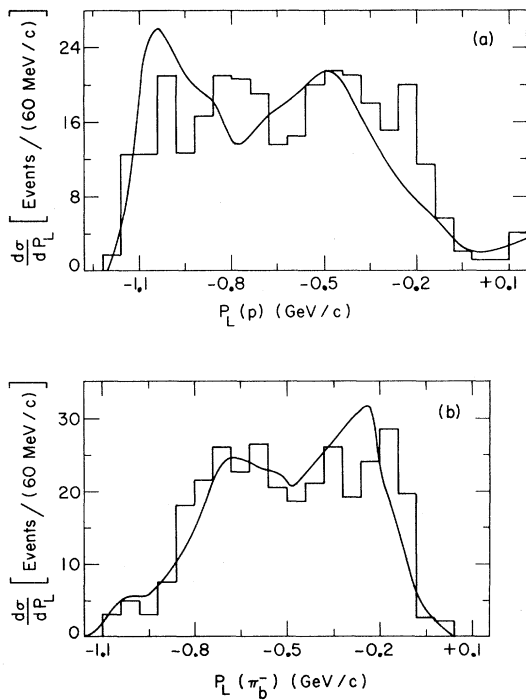


FIG. 5. Comparison of baryon-exchange model and data, seven cuts: Distribution as a function of (a) longitudinal momentum of the proton, and (b) longitudinal momentum of  $\pi_b^-$ .

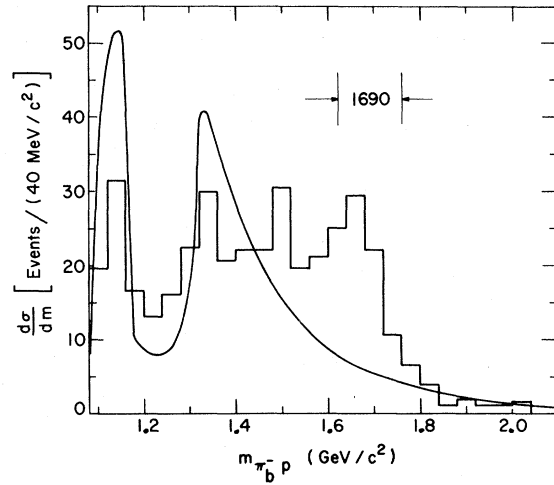


FIG. 6. Distributions in the invariant mass of the  $(\pi_b^-p)$  system. The  $N^*(1690)$  region is shown by the vertical lines. Six cuts have been applied here.

parent discrepancy in  $P_L(p)$  is due entirely to events in the  $\Delta^0(1236)$  region; elimination of this region by a straight mass cut, as opposed to a window cut, brings the model and data into agreement. The slope of the  $\cos\theta_{pp}$  distribution was of course fitted by adjusting the scale parameter  $S_2$ . These essentially angular variables are primarily single-particle variables, such as might be measured in a single-particle inclusive experiment ( $\cos\theta_{pp}$  is, however, measured in the  $\pi^-p$  center-of-mass system, and is thus determined by the momenta of these *two* particles). The  $\pi^-p$  mass, on the other hand, is clearly a crucial two-particle variable which must be properly treated by a realistic model. Our model, as shown in Fig. 6, does a poor job of describing this mass distribution, as should be expected *a priori*. The data have a broad shape, as does phase space, with distinct resonance peaks at 1236 MeV (see Fig. 7), 1520 MeV (perhaps), and 1690 MeV. The baryon-exchange model, in contrast, has a typically peaked structure, which could be somewhat broadened by a further increase in  $S_2$ , but which could not possibly be adjusted to satisfactorily describe the general shape of the data. Even when we attempt to remove the more prominent resonances [ $\Delta^0(1236)$  and  $N(1690)$ ], there still remain irreconcilable differences between model and data.

The model does an adequate job of fitting distributions which include the  $\rho$  or its decay products, but we do not show these since they are not our main interest. The fits are quite similar in quality to those obtained with the phase-shift model, which will be presented in Sec. IV.

Since it appears that single-particle distributions

may be well fitted by this model in spite of the poor fit of the  $\pi^- p$  mass, we looked at a larger sample of data, to see if this persisted. After removing the restrictions on  $m(\pi^- p)$  and  $u$ , we have a sample of data which consists of all events with backward protons, a peripheral  $\rho^0$ , and no  $\Delta^{++}$ . This is the largest sample our model could be associated with, and we should expect to fit the single-particle distributions in this sample, if we wish to draw any larger conclusions than we have so far. The results are summarized in Fig. 7. We find, in fact, that it is possible to roughly fit the distributions in  $\cos\theta_{pp}$ ,  $P_L(p)$ , and  $P_L(\pi_b^-)$ , among others. However, it is necessary to readjust our parameters  $S_1$  and  $S_2$  in order to achieve such a fit. The mass plot ( $m_{\pi^- p}$ ) falls too rapidly, as before. We conclude that the baryon-exchange model is able to describe single-particle distributions for *general* backward proton events, in spite of its failure to describe the basic over-all structure of the data. We speculate that such behavior might hold true in other multiparticle processes and, by extension, in inclusive processes. In particular, it is certainly possible to change certain

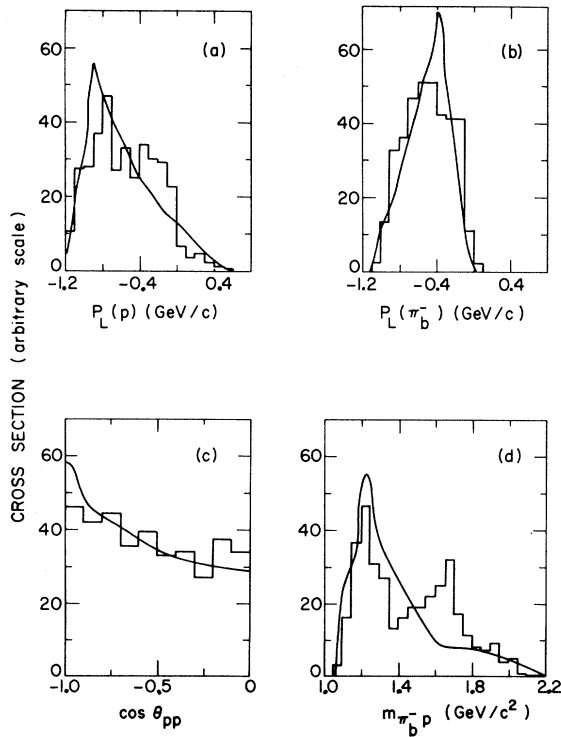


FIG. 7. Comparison of baryon-exchange model and data with four cuts (see text): Cross section as a function of (a) longitudinal momentum of the proton, (b) longitudinal momentum of  $\pi_b^-$ , (c)  $\cos\theta_{pp}$ , and (d)  $(\pi_b^- p)$  invariant mass.

details (Regge trajectories and residues, for example) of our model in order to improve the agreement with the longitudinal-momentum distributions of Figs. 5 or 7.

#### IV. PHASE-SHIFT MODEL

The Reggeized-baryon-exchange model fitted the  $m(\pi^- p)$  spectrum rather poorly due to the persistence of resonances in the  $\pi^- p$  system despite the stringent cuts. A more realistic model would be one which takes into account explicitly the presence of resonances in the  $\pi^- p$  effective mass. A simple model of backward scattering was devised to take resonance formation into account in an inherently dual way. The proton-(Reggeized) pion scattering amplitude (lower vertex in Fig. 1) was parametrized in terms of the appropriate  $\pi^- p$  on-shell phase shifts. The CERN theoretical phase shifts<sup>10</sup> for partial waves up to and including  $G$  waves were used to calculate the  $\pi^- p$  amplitude.  $X$  in Fig. 1 is again a  $(\pi^+ \pi^-)$  system in the  $\rho$  region. The  $(\pi^+ \pi^-)$  amplitude was chosen to be the sum of a constant (to account for the background) and the  $p$ -wave amplitude. The  $p$ -wave amplitude was taken to have a Breit-Wigner form with energy-dependent width as described in the previous model. The exchanged particle was again taken to be a Reggeized pion, but in this model  $S_1 = 2.0 \text{ GeV}^2$ . The cuts for this model are

$$\begin{aligned} \cos\theta_{pp} &\leq 0.0, \\ -1.0(\text{GeV}/c)^2 &\leq t \leq 0.0(\text{GeV}/c)^2, \\ 0.65 \text{ GeV} &\leq m(\pi^+ \pi^-) \leq 0.85 \text{ GeV}, \end{aligned}$$

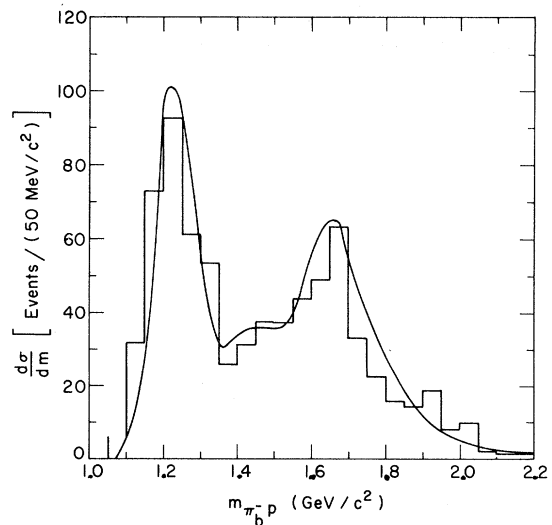


FIG. 8. Comparison of phase-shift model and data: Distribution as a function of  $(\pi_b^- p)$  invariant mass. Four cuts have been applied.

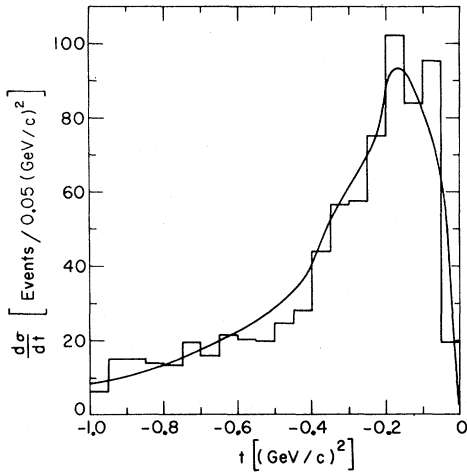


FIG. 9. Comparison of the phase-shift model and data, four cuts: Distribution as a function of  $t$ .

and no  $\Delta^{++}(1236)$ . The model is again normalized to the data, which now consist of 744 events.

The over-all fit of the model to the data is quite good. The major shortcoming of the baryon-exchange model has now been overcome; the fit to the  $m(\pi^-p)$  spectrum in the backward region is excellent (Fig. 8). The distributions in  $t$  and  $u$  are very well fitted (Figs. 9, 10) by our choice of the single parameter  $S_1$ . The remaining distributions are also well reproduced by the model (Figs. 11–13) with the possible exception of the  $\cos\theta_{pp}$  plot (Fig. 11). This plot shows a peaking in the model around  $-0.9$  which is apparently absent in the data. The absence of data in this region may be a statistical effect. When the sample of data was increased to 1170 events by including 7.0-GeV/ $c$  data, a small peak was observed in this region. The other

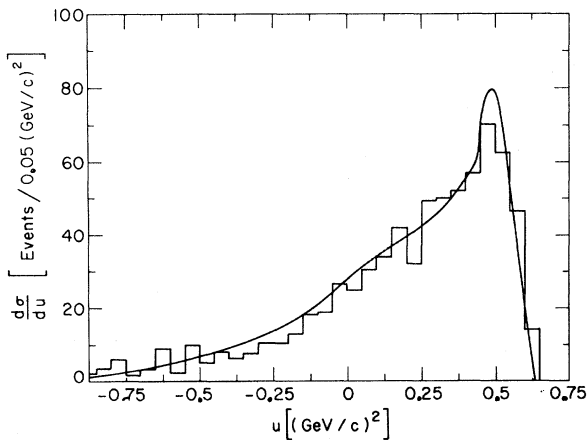


FIG. 10. Comparison of the phase-shift model and data, four cuts: Distribution as a function of  $u$ .

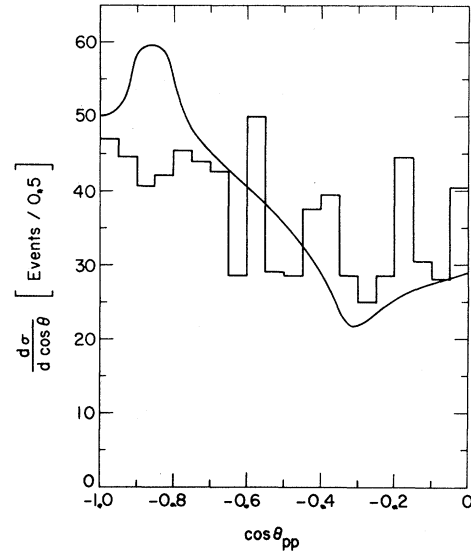


FIG. 11. Comparison of the phase-shift model and data, four cuts: Distribution as a function of  $\cos\theta_{pp}$ .

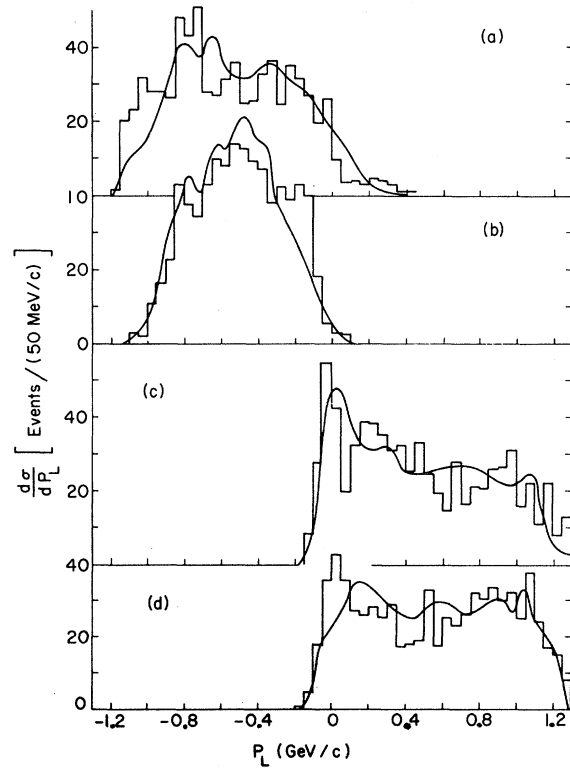


FIG. 12. Comparison of the phase-shift model and data, four cuts: Distribution as a function of the longitudinal momentum of (a) the proton, (b)  $\pi^-$ , (c)  $\pi^+$ , and (d)  $\pi^-$ .

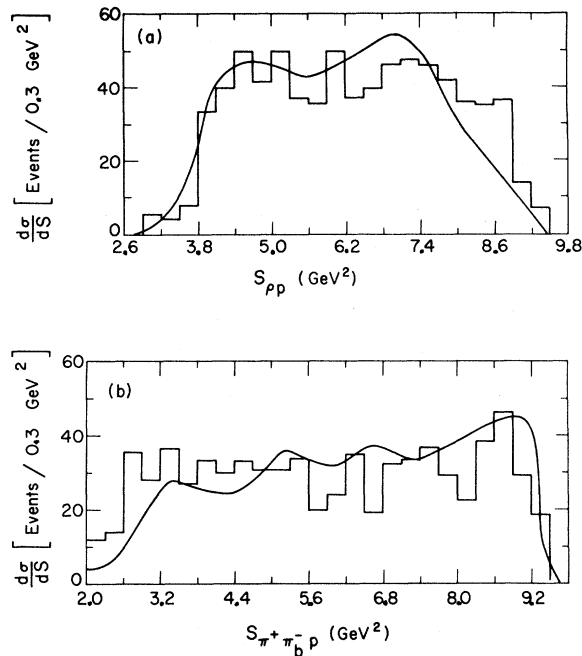


FIG. 13. Comparison of the phase-shift model and data. Four cuts. Distribution vs. three-particle invariant masses: (a)  $S_{\rho p} = (q_1 + q_2 + q_3)^2$ , and (b)  $S_{\pi^+ \pi_b^- p} = (q_2 + q_3 + q_4)^2$ .

graphs are not altered significantly by this addition.

The longitudinal-momentum distributions (Fig. 12) are well fitted by the model over-all, but the proton and the  $\pi_b^-$  distributions do show excess events around  $-1.0$  GeV/c and  $-0.2$  GeV/c, respectively. A cut on  $m(\pi^-p)$  shows that these events come almost exclusively from the region  $m(\pi^-p) \leq 1.2$  GeV.

Note, finally, that we fit the three-particle sub-energies,  $S_{\rho p}$  and  $S_{\pi^+ \pi_b^- p}$ , rather well too (Fig. 13). It is possible that some of the small wiggles in the theoretical curves of Figs. 12 and 13 are actually due merely to the limited statistical accuracy of our Monte Carlo generation.

As expected, this model on the whole gives a better description of the data than the baryon exchange does. It does a reasonably good job of fitting the individual particle distributions (longitudinal momenta) as well as the combined particle distributions (effective masses).

## V. CONCLUSIONS

The parametrization of the data in terms of single-pion exchange at the upper ( $\rho$ ) vertex seems to work well for both models. The scale parameter  $S_2$  required by the phase-shift model is closer to the usual value of  $1.0$  GeV<sup>2</sup>. The major differ-

ences between the models are to be found in their predictions of the shape of the two-particle distributions at the lower ( $\pi^-p$ ) vertex.

The Reggeized-baryon-exchange model fits the individual particle distributions (longitudinal momenta) fairly well. However, it gives a good fit to the effective-mass distribution in only a small portion [perhaps  $1.08 \text{ GeV} \leq m(\pi^-p) \leq 1.3 \text{ GeV}$ ] of the total spectrum. The success of this model in describing the nonperipheral events in inclusive reactions would thus seem to be due to the relative insensitivity of the single-particle distributions to the details of the model.

The fact that baryon exchange does fit single-particle distributions over a wide range of energies<sup>2</sup> is certainly evidence in support of the model. It also appears to indicate that a dual interpretation of Reggeized baryon exchange is valid. Our results indicate that the model would fail in an attempt to describe multiparticle correlations. But it must be stressed that we have looked only at a small portion of data from an exclusive process. The possibility remains that the effects we observe might get washed out when one sums (experimentally) the contributions from many different processes.

The phase-shift model gives a good over-all fit to the data. The fit is even better than might be expected since the on-shell phase shifts were used to describe an off-shell reaction. The failure of the simple Reggeized-baryon-exchange model and the success of the more highly structured phase-shift model merely point up the fact that the nonperipheral events are formed by mechanisms more complicated (e.g., resonance formation) than exchange of a single trajectory. The success of the baryon-exchange model in describing single-particle distributions but not the effective-mass distribution emphasizes the importance of looking at correlation functions for inclusive reactions to check the validity of models of high-energy scattering processes.

## ACKNOWLEDGMENTS

We are indebted to U. Kruse for kindly providing us with a copy of the Illinois data, and to Philip Coulter for discussions on this work. We gratefully acknowledge the support of the University of Alabama Research Grants Committee in providing us with financial aid during the time this work was carried out. We also wish to acknowledge the generous support of the University of Alabama Computing Center, which is supported in part by NSF Grant No. GJ-212.

\*This work was supported in part by a grant from the Research Grants Committee of the University of Alabama.

<sup>1</sup>C. W. Akerlof *et al.*, Phys. Rev. D **3**, 645 (1971); J. V. Allaby *et al.*, CERN Report No. 70-12, 1970 (unpublished); E. W. Anderson *et al.*, Phys. Rev. Letters **19**, 198 (1967).

<sup>2</sup>L. Caneschi and A. Pignotti, Phys. Rev. Letters **22**, 1219 (1969); C. Risk and J. Friedman, *ibid.* **27**, 353 (1971).

<sup>3</sup>S. D. Drell, D. J. Levy, and T.-M. Yan, Phys. Rev. Letters **22**, 744 (1969); Phys. Rev. **187**, 2159 (1969); Phys. Rev. D **1**, 1035 (1970); S.-S. Shei and D. M. Tow, Phys. Rev. Letters **26**, 470 (1971).

<sup>4</sup>Z. Ajduk, L. Michejda, and W. Wojcik, Acta. Phys. Polon. **A37**, 93 (1968).

<sup>5</sup>Chan Hong-Mo, J. Loskiewicz, and W. W. M. Allison, Nuovo Cimento **57A**, 93 (1968).

<sup>6</sup>We are grateful to U. Kruse for providing us with the

4-vector tapes arising from two separate experiments. The first of these resulted from an exposure in the Lawrence Radiation Laboratory 72-in. bubble chamber, and the second from an exposure in the SLAC 82-in. chamber. For other descriptions of these data, see B. Terreault, Ph.D. thesis, University of Illinois, 1969 (unpublished); G. Ascoli, H. B. Crawley, U. Kruse, D. W. Mortara, E. Shafer, A. Shapiro, and B. Terreault, Phys. Rev. Letters **21**, 113 (1968); G. Ascoli, D. V. Brockway, H. B. Crawley, L. B. Eisenstein, R. W. Hanft, M. L. Ioffredo, and U. Kruse, *ibid.* **25**, 962 (1970).

<sup>7</sup>J. D. Jackson, Nuovo Cimento **34**, 1644 (1964).

<sup>8</sup>E. L. Berger and G. Fox, Nucl. Phys. **B26**, 1 (1971).

<sup>9</sup>S. T. Jones, Phys. Rev. D **2**, 856 (1970).

<sup>10</sup>D. J. Herndon, A. Barbaro-Galtieri, and A. H. Rosenfeld, LBL Report No. UCRL-20030, 1970 (unpublished).

PHYSICAL REVIEW D

VOLUME 6, NUMBER 9

1 NOVEMBER 1972

## Systematics of Single-Particle Spectra in Proton-Proton Collisions\*

M. Jacob†

*National Accelerator Laboratory, P. O. Box 500, Batavia, Illinois 60510*

and

R. Slansky and C.-C. Wu‡

*Physics Department, Yale University, New Haven, Connecticut 06520*

(Received 26 July 1972)

The shapes and scaling characteristics of the  $\pi^\pm$ ,  $K^\pm$ ,  $p$ ,  $n$ ,  $\bar{p}$ , and  $\Lambda$  spectra in proton-proton collisions may be easily understood in terms of the clustering effects observed in hadron production at present machine energies. This is the general basis for the success of the nova model. Good quantitative agreement between the model distributions and the experimental data is found.

### I. INTRODUCTION

Many inclusive cross sections have now been measured, including the momentum distributions of  $\pi^\pm$ ,  $K^\pm$ ,  $p$ ,  $\bar{p}$ , and  $\Lambda$  in proton-proton collisions for different incident proton energies.<sup>1-10</sup> The two aspects of the systematics of these inclusive single-particle distributions which have attracted the most attention are their shapes and scaling characteristics. Although at first sight the variety of experimental observations appears puzzling, this variation results from a common type of production mechanism. The observed differences in distribution shapes and scaling properties reflect the nature (mass and quantum numbers) of the observed particle more than the details of the production process. Our purpose is to show that the differences can be easily understood in terms of kinematical rather than dynamical properties, once some general properties of production processes

are accepted.

The variables we shall use for describing the inclusive distributions are the center-of-mass energy  $W = \sqrt{s}$ , the Feynman scaling variable  $x = 2k_L/\sqrt{s}$  (where  $k_L$  is the center-of-mass longitudinal momentum of the observed particle), and the transverse momentum squared  $k_T^2$ .<sup>11</sup> The Lorentz-invariant inclusive distribution is written as

$$f(x, k_T^2, s) = \frac{2\omega_k}{\pi\sqrt{s}} \frac{d^2\sigma}{dxdk_T^2}, \quad (1)$$

where  $\omega_k$  is the center-of-mass energy of the selected secondary. Only proton-proton collisions are considered in this paper.

The observed shapes of  $f(x, k_T^2, s)$  in  $x$  for fixed  $k_T^2$  and  $s$  vary considerably.<sup>9</sup> For example, in proton-proton collisions, we may contrast the pion distributions,<sup>1-5</sup> which fall almost exponentially in  $x$  (or  $x^2$  with an average value of  $x$  as low as 0.1), with the  $\Lambda$  distribution, which rises gently from